

# UC Merced

## UC Merced Previously Published Works

### Title

Accelerated Neuronal Differentiation Toward Motor Neuron Lineage from Human Embryonic Stem Cell Line (H9)

### Permalink

<https://escholarship.org/uc/item/2k3518st>

### Journal

Tissue Engineering Part C Methods, 21(3)

### ISSN

1937-3384

### Authors

Lu, David  
Chen, Eric YT  
Lee, Philip  
[et al.](#)

### Publication Date

2015-03-01

### DOI

10.1089/ten.tec.2013.0725

Peer reviewed

# Accelerated Neuronal Differentiation Toward Motor Neuron Lineage from Human Embryonic Stem Cell Line (H9)

David Lu, MS,<sup>1,\*</sup> Eric Y.T. Chen, PhD,<sup>1-3,\*</sup> Philip Lee, BS,<sup>1</sup> Yung-Chen Wang, BS,<sup>1</sup>  
Wendy Ching, BS,<sup>1</sup> Christopher Markey, BS,<sup>1</sup> Chase Gulstrom, BS,<sup>1</sup>  
Li-Ching Chen, PhD,<sup>4</sup> Thien Nguyen, MD, PhD,<sup>5</sup> and Wei-Chun Chin, PhD<sup>1</sup>

Motor neurons loss plays a pivotal role in the pathoetiology of various debilitating diseases such as, but not limited to, amyotrophic lateral sclerosis, primary lateral sclerosis, progressive muscular atrophy, progressive bulbar palsy, pseudobulbar palsy, and spinal muscular atrophy. However, advancement in motor neuron replacement therapy has been significantly constrained by the difficulties in large-scale production at a cost-effective manner. Current methods to derive motor neuron heavily rely on biochemical stimulation, chemical biological screening, and complex physical cues. These existing methods are seriously challenged by extensive time requirements and poor yields. An innovative approach that overcomes prior hurdles and enhances the rate of successful motor neuron transplantation in patients is of critical demand. Iron, a trace element, is indispensable for the normal development and function of the central nervous system. Whether ferric ions promote neuronal differentiation and subsequently promote motor neuron lineage has never been considered. Here, we demonstrate that elevated iron concentration can drastically accelerate the differentiation of human embryonic stem cells (hESCs) toward motor neuron lineage potentially via a transferrin mediated pathway. HB9 expression in 500 nM iron-treated hESCs is approximately twofold higher than the control. Moreover, iron treatment generated more matured and functional motor neuron-like cells that are ~1.5 times more sensitive to depolarization when compared to the control. Our methodology renders an expedited approach to harvest motor neuron-like cells for disease, traumatic injury regeneration, and drug screening.

## Introduction

**M**OTOR NEURON LESIONS occur in conditions such as stroke, traumatic brain injury, and motor neuron diseases, which can result in weakness, immobility, and mortality.<sup>1,2</sup> Unfortunately, the paucity of effective medicinal treatment and the inability to repair motor axons renders the path toward regeneration seemingly insurmountable. Hampered by limited therapeutic options, current strategies aim to reestablish damaged connections/functions and transplant with derived motor neurons.<sup>2-4</sup> As a result, stem cell therapy is being developed as a potential new avenue to ameliorate the pathology. Traditionally, motor neuron derivation protocols call for multistep procedures from human embryonic stem cells (hESCs) in more than 30 days. These complicated processes necessitate generation of neuralepithelial cells in ~2 weeks followed by 4–6 weeks of motor neuron differ-

entiation. Reinforcing the cumbersome nature, long-term incubation with a myriad of chemicals, growth factors and excessive transcriptional activators such as, but not limited to, purmorphamine, cAMP, retinoic acid (RA), sonic hedgehog (SHH), fibroblast growth factors (FGFs), nerve growth factor (NGF), brain-derived neurotrophic factor (BDNF), glial-derived neurotrophic factor, and insulin-like growth factor-1 (IGF-1) are indispensable, in addition to modifying oxygen level during culture.<sup>5-10</sup> It does, however, appear that biochemical contributions have reached a plateau in advancing motor neuron differentiation, which has subsequently spawned an array of investigations on alternative stimulations.

In recent years, a growing body of evidence has attributed motor neuron differentiation and maturation to physical signals. Recently, attention has been directed toward micro- and nano-architectures such as geometry of extracellular

<sup>1</sup>Bioengineering Program, School of Engineering, University of California, Merced, California.

<sup>2</sup>Biomedical Engineering Research Center, Chang Gung University, Tao-Yuan, Taiwan.

<sup>3</sup>MicroBase Technology Corp, Bade City, Taoyuan, Taiwan.

<sup>4</sup>Taipei Medical University–Shuang Ho Hospital, Ministry of Health and Welfare, Division of Gastroenterology and Hepatology, Taipei Medical University, Taipei, Taiwan.

<sup>5</sup>Department of Neurology, The Johns Hopkins University, Baltimore, Maryland.

\*These authors equally contributed to this work.

matrices, patterns, grooves, and alignments that promote survival, growth, processes of neuritogenesis, and polarity formation of motor neurons. For instance, both aligned and randomly orientated poly-L-lactic acid (PLLA) electrospun nanofibers significantly accelerated the spinal motor neuron neuritogenesis and major neurite development compared with flat surface without engineered topography.<sup>11</sup> Other factors influencing motor neuron growth includes surface functionalization since polyanionic film had been demonstrated to enhance neuritic arborization and length of motor neurons.<sup>12</sup> Despite the positive effects of biophysical cues in motor neuron differentiation and development, costly small-scale fabrication severely hinders stem cell-derived motor neuron transplantation as a feasible therapy or a potential clinical application. Therefore, more economical and efficient strategies to accelerate motor neuron differentiation and functional maturity are very much in need.

In addition to both biological and topographical stimulations, various ions had been demonstrated to critically influence cellular proliferation, homeostasis, and degeneration.<sup>13–18</sup> The question of whether a simple modification in ionic concentration can modulate regeneration by promoting neuronal differentiation toward motor neuron lineage has not, heretofore, been considered. Iron is fundamentally required by all mammalian cells for DNA synthesis, DNA repair, proliferation, oxygen transport, electron transfer, neurotransmitter metabolism, and mitochondrial energy production.<sup>19,20</sup> Iron concentrations in the cerebral cortex, cerebellum-pons, and midbrain are at their highest immediately after birth. It is crucial for myelination, neurotransmitter synthesis, synaptogenesis, and neuronal development and function.<sup>21</sup> While ferric and ferrous forms are widely distributed in the rat brain, they are concentrated in areas such as the globus pallidus, basal ganglia, amygdaloid body, cerebellar nuclei, red nucleus, vestibular nuclei, and trigeminal motor nucleus.<sup>21</sup> Iron rapidly accumulates in these areas during neural development, suggesting its participation in behavioral organization and motor activities. In fact, some neurons specifically involved in the motor system contain high level of ferric and ferrous ions, and iron regulatory proteins in axons, cytoplasm, and lysosomes.<sup>21</sup> Coincidentally, iron deficiency is strongly correlated with adverse effects on brain function including cognitive impairments, learning impairments, and motor deterioration in infants and young children.<sup>22,23</sup> For instance, iron insufficient rats traveled significantly slower in the elevated plus maze and fell off rotarod faster than control rats indicating damaged motor functions.<sup>24</sup> Iron-deficient humans (especially during childhood) also show decreased physical activity, weakened skeletal motor performance, and motor impairments such as restless legs syndrome.<sup>24–26</sup> In addition to modulating motor activities, iron regulates cellular energy metabolism and ATP production.<sup>27</sup> Cellular energy is a critical controller of proliferation rate, self-renewal, and differentiation. Neurons and axons maintain high levels of iron to support a continuous demand for high metabolic activities. Experiments have also shown that iron treatment increased generation of oligodendrocytes from glial precursors.<sup>27</sup> Additionally, during neuronal differentiation, mitochondrial biogenesis coupled with ATP production support neurite outgrowth.<sup>28</sup> Hence, increasing iron availability may be providing the energy needed for neuronal differentiation; how-

ever, whether iron can promote motor neuron differentiation remains an enigma.

Currently available motor neuron differentiation approaches rely on stimulations from biochemical and physicochemical means, little is known whether iron may provide additional improvement for the existing methods. Since iron exerts crucial influence on neural physiology and the lack of which leads to morbidity, we examined the ability of iron to facilitate neural differentiation toward motor neuron lineage and the mechanism involved.

## Materials and Methods

### *hESC culture*

hESC lines H9 from Wicell (passage 30–50) were cultured in 20% knockout (KO) serum replacement medium on mitomycin C (Sigma-Aldrich)-treated mouse embryonic fibroblasts (MEFs).<sup>29–32</sup> The standard 20% KO serum replacement medium contained 20% KO serum replacement (Invitrogen), 1% nonessential amino acids (Invitrogen), 1 mM L-glutamine (Invitrogen), Dulbecco's modified Eagle's medium (DMEM/F12; Invitrogen), 0.1 mM b-mercaptonethanol (Sigma-Aldrich), and 4 ng/mL FGF-2 (Sigma-Aldrich). The medium was changed every day and hESCs were passed every 7 days.

### *Embryoid body formation*

hESC colonies were treated with dispase (0.5 mg/mL; Invitrogen) to remove colonies from MEF feeder layer. The colonies were cultured in an ultra-low attachment dish (Costar, Fisher) for 5 days in 20% KO serum replacement medium without FGF-2 to form embryoid bodies (EBs).

### *Iron supplement*

To allow attachment, EBs were transferred to wells coated with PLO and Laminin<sup>30,32</sup> and subsequently incubated with N2 medium supplement consisting of DMEM/F12, non-essential amino acids, sodium pyruvate (Invitrogen), N2 supplement (Invitrogen), 0.1 mM b-mercaptonethanol (Sigma-Aldrich), and FGF-2 (8 ng/mL). For experimental purpose, EBs were treated with N2 medium containing iron (III) chloride at various concentrations (100 nM, 500 nM, and 1  $\mu$ M) (Sigma-Aldrich) for a maximum of 14 days. At day 5 of differentiation, N2 medium was replaced with Neural-basal media containing 2 M L-glutamine, 2% B27 serum-free supplement, and 25 ng/mL NGF to further the maturation of neural-like colonies for an additional 3 days.<sup>33</sup> Samples were then fixed for immunofluorescent staining or collected for western blot analysis.

### *Immunocytochemistry*

Adherent cells were rinsed with Hank's solution and fixed with 4% paraformaldehyde (Sigma-Aldrich) for 20 min. Cells were treated with 0.1% Triton X-100 (Sigma-Aldrich) and 1% bovine serum albumin for 30 min before they were incubated at 4°C overnight in primary antibodies  $\beta$ -III tubulin (1:500; Millipore), Peripherin (1:200; Santa Cruz), choline acetyltransferase (ChAT, 1:200; Millipore), microtubule-associated protein 2 (MAP2, 1:500; Millipore), NeuN (1:200; Millipore), neurofilament (NF, 1:1000; Millipore), synapsin (1:500; Millipore), and HB9 (motor neuron-specific transcription

factor, 1:500; Santa Cruz). Secondary fluorescent antibodies were used at 1:500 for 1 h at room temperature (AlexaFluor 488 and Cy3; Invitrogen), cell nuclei were stained with DAPI (1:5000). Cell imaging obtained using same exposure time for image acquisitions in each group. Images were acquired by Nikon Eclipse TE2000-U fluorescent microscope (Nikon Eclipse TE2000-U).

#### Image analysis

**Quantification of the axonal length.** Axonal length was quantified in accord to our protocol published previously.<sup>30</sup> In brief, more than 20 fluorescently stained axons were measured at random from each of ~10 EBs. Axons were measured (in pixels using NIS-Elements software) from the tip of axons to the end and averaged. Micron beads (F13838; Invitrogen) were used for calibration converting pixel to length (mm) of axons. The results were obtained using the NIS-ELEMENTS software (Nikon Instruments).

**Quantification of the axonal density.** Axonal density was quantified in accordance with our previously published protocol.<sup>30</sup> In short, axonal density was assessed by quantifying the total fluorescence intensity of axons using random placement of more than 30 defined regions of interest. Axonal density was measured from more than 10 EBs in pixels and analyzed with NIS-ELEMENTS software. Final ratios were derived by dividing total intensity of axons cultured with iron additive by that of the controls. Because the cells were subjected to the same staining conditions and assessment procedures, potential inconsistencies in fluorescence intensity could be counteracted.

#### Western blot

Neuronal differentiated stem cells were harvested and lysed. A total of 50 µg of protein was loaded into each well and subsequently resolved on 10% SDS-PAGE gel with a 5% stacking SDS-PAGE. Proteins were transferred onto Immobilon-P Membrane (PVDF; Millipore) overnight at 4°C. The membranes were blocked in 5% nonfat milk and hybridized with primary antibodies including β-III tubulin (1:1000; Millipore), peripherin (1:1000; Santa Cruz Biotechnology, Inc.), NeuN (1:1000; Millipore), and GAPDH (1:10,000; Millipore). Membranes were then rinsed with TBST, incubated with secondary antibodies (goat anti-mouse, donkey anti-goat, and goat anti-rabbit HRP; Millipore) and developed with SuperSignal West Pico Chemiluminescent Substrate (Thermo Scientific). Images were taken with ChemiDoc XRS (Bio-Rad Laboratories, Inc.) and analyzed with Quantity One software (Bio-Rad Laboratories, Inc.).

#### Neural functional assay

Neural functional assay was measured by testing for depolarizing-dependent synaptic vesicle recycling in accord to our previously established protocol.<sup>30</sup> In brief, cells were carefully rinsed with DPBS, loaded with FM1-43 dye (2 µM) ( $\lambda_{\text{Ex}} = 510$  nm and  $\lambda_{\text{Em}} = 626$ ) (Invitrogen) for 5 min, and were carefully rinsed again. Exocytosis of synaptic vesicles was triggered by 50 µM glutamic acid, 200 µM acetylcholine (ACh), or depolarizing solution (high K<sup>+</sup>) (in mM: 20.9 NaCl, 100 KCl, 1.2 MgCl<sub>2</sub>, 1.2 NaH<sub>2</sub>PO<sub>4</sub>, 1.2

Na<sub>2</sub>SO<sub>4</sub>, 2.5 CaCl<sub>2</sub>, 25 NaHCO<sub>3</sub>, and 10 glucose, pH 7.3; Sigma-Aldrich). Data were collected with Nikon Eclipse TE2000-U microscope with heated stage controlled at 37°C.

#### Acquisition of granular pH

Granular pH of EBs was monitored by loading EBs with 1 µM of LysoSensor™ Green DND-189 ( $\lambda_{\text{Ex}} = 443$  nm and  $\lambda_{\text{Em}} = 505$ ) (Invitrogen) for 30 min.<sup>30</sup> LysoSensor Green DND-189 was carefully rinsed with Tyrode solution. Granular fluorescence was captured using Nikon Eclipse TE2000-U. The images were analyzed with Simple PCI software (Compix, Inc., Imaging Systems).

#### Iron uptake disruption

A modification from prior published protocol was used to disrupt transferrin acidification.<sup>34</sup> Methylamine hydrochloride (100 µM) was added to the culture medium and cultured in the same fashion with varying iron concentrations. Methylamine is a known blocker of transferrin-iron release through their lysosomotropic properties.

#### Statistical analysis

The data were presented as mean ± SD. Each experiment was performed independently at least three times. Statistical significance was determined using a Student's *t*-test analysis with *p*-values of <0.005 (Microsoft Excel and GraphPad Prism 4.0; GraphPad Software, Inc.).

## Results

### *Elevated iron concentration accelerated neuronal differentiation from hESCs*

We examined whether higher iron concentration can accelerate neuronal differentiation and maturation. Conventional protocol uses basal neural differentiation (N2) medium (with existing 1.5 µM of basal iron) to promote differentiation.<sup>5,31,32</sup> To test the hypothesis, hESC EB was supplemented with 0.1–1 µM FeCl<sub>3</sub> in N2 medium. Iron-instigated accelerated differentiation toward neural lineage was assessed by measuring axonal extension (length) and density of fluorescently labeled β-III tubulin (Fig. 1) and peripherin antibodies (Fig. 2). These two biomarkers signify matured axonal development during neuronal differentiation.<sup>7,8,35</sup> Elevating iron concentrations increased axonal length and density from day 2 to 8 of differentiation (Fig. 1). Major differences between the control and iron-enriched groups were observed after 5 days of differentiation. The axonal lengths were enhanced by ~1.52×, 1.61×, and 1.76× when compared with the control, at 0.1, 0.5, and 1 µM of FeCl<sub>3</sub>, respectively (Fig. 1B). Simultaneously, augmenting iron levels distinctly improved axonal density by ~1.35-, 1.5-, and 1.48-folds at 0.1, 0.5, and 1 µM of FeCl<sub>3</sub>, respectively (Fig. 1C). Axonal growth reached a plateau after 11 days of differentiation (Figs. 1 and 2). A commensurate increase in axonal length and density was also independently confirmed with peripherin staining (Fig. 2). Our data suggested that higher iron concentrations can accelerate neuronal differentiation by enhancing axonal sprouting and elongation in a dose-dependent fashion throughout 2–8 days of differentiation.

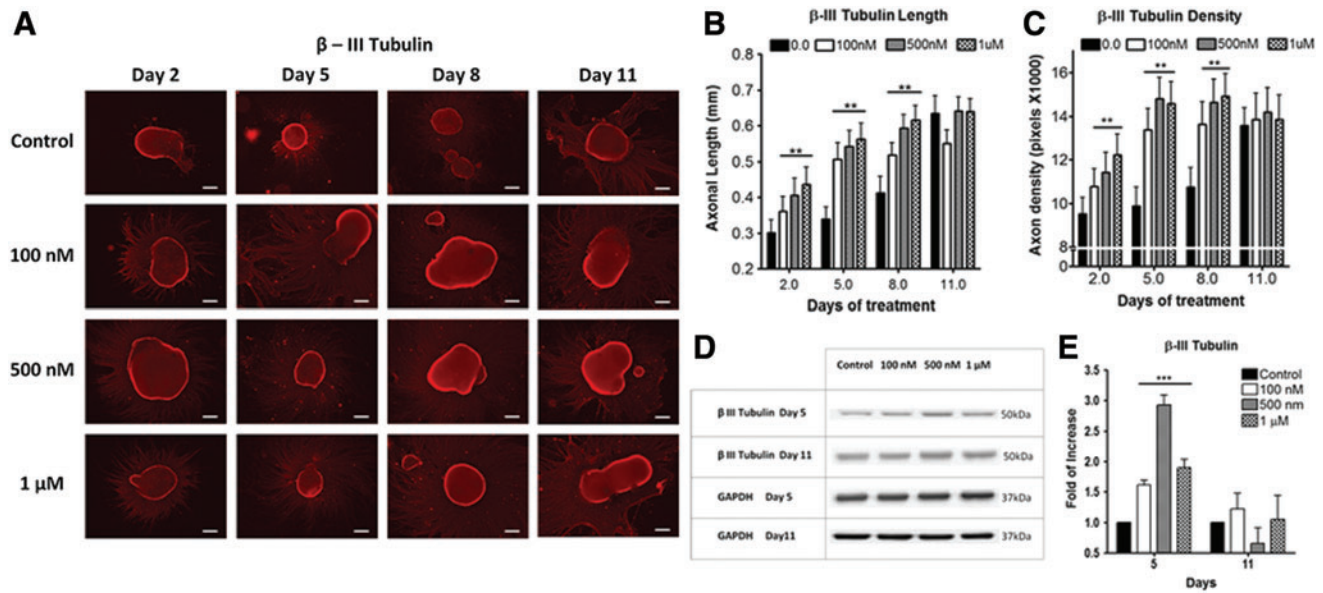


**FIG. 1.** Human embryonic stem cells (hESCs)-derived neuronal progenitor with varying additive  $\text{Fe}^{3+}$ . (A) Immunofluorescence of  $\beta$ -III tubulin staining of the control (nonadditive  $\text{Fe}^{3+}$ ), 100 nM, 500 nM, and 1  $\mu\text{M}$   $\text{Fe}^{3+}$  at 2, 5, 8, and 11 days of differentiation (red; scale bar = 200  $\mu\text{m}$ ). Analysis of (B) axonal length (mm) and (C) density of  $\beta$ -III tubulin with varying concentrations of  $\text{Fe}^{3+}$  at 2, 5, 8, and 11 days of differentiation ( $n \geq 100$ ,  $**p < 0.005$ ). (D) Western blot of  $\beta$ -III tubulin with (E) quantitative analysis of  $\beta$ -III tubulin protein expression fold of increase for 5 and 11 days of differentiation ( $n \geq 3$ ,  $***p < 0.001$ ). Color images available online at [www.liebertpub.com/tec](http://www.liebertpub.com/tec)

In addition to morphological changes, western blotting was conducted to quantitatively assess key neuronal biomarkers for accelerated differentiation. Analysis of global cellular expression of  $\beta$ -III tubulin and peripherin showed that the optimal neuronal differentiation occurred at day 5.

After 5 days of differentiation,  $\beta$ -III tubulin expression levels were notably elevated by about 1.6-, 3.0-, and 2.0-folds at 0.1, 0.5, and 1  $\mu\text{M}$  of  $\text{FeCl}_3$ , respectively (Fig. 1D, E). After 11 days of differentiation, both neuronal markers revealed no significant differences between iron-enriched

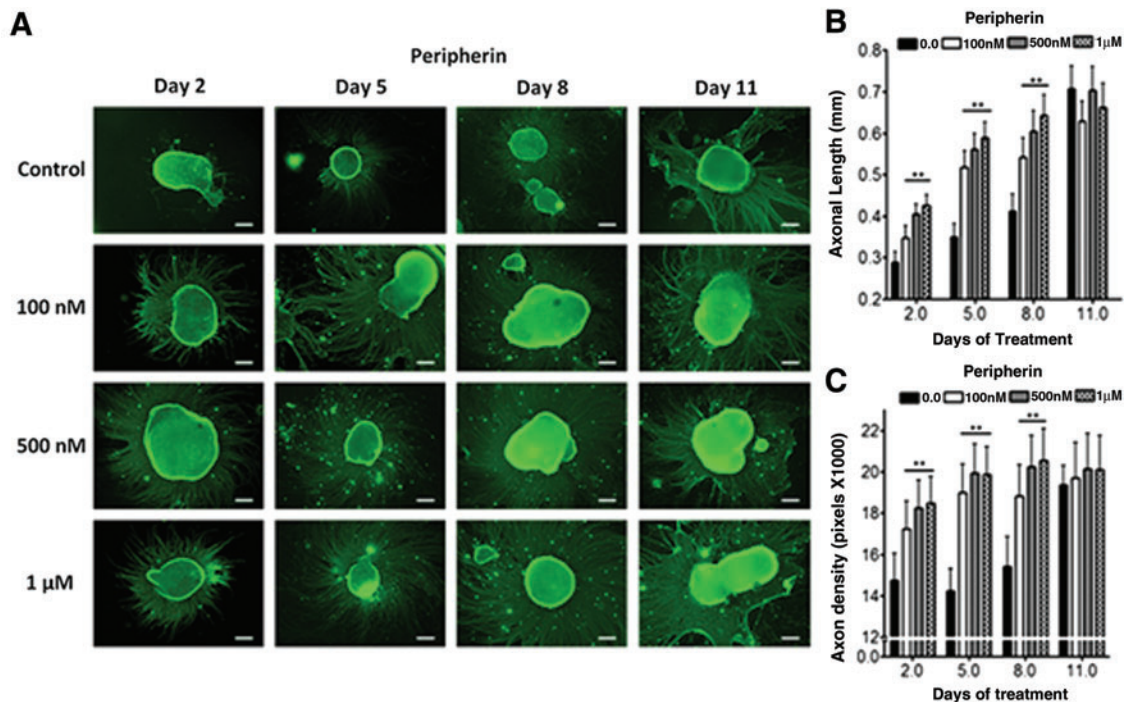


**FIG. 2.** hESC-derived neuronal progenitor with varying additive  $\text{Fe}^{3+}$ . (A) Immunofluorescent of peripherin staining control (nonadditive  $\text{Fe}^{3+}$ ), 100 nM, 500 nM, and 1  $\mu\text{M}$   $\text{Fe}^{3+}$  at 2, 5, 8, and 11 days of differentiation (scale bar = 200  $\mu\text{m}$ ). Analysis of (B) axonal length (mm) and (C) density of peripherin with varying concentrations of  $\text{Fe}^{3+}$  at 2, 5, 8, and 11 days of differentiation ( $n \geq 100$ ,  $**p < 0.005$ ). Color images available online at [www.liebertpub.com/tec](http://www.liebertpub.com/tec)

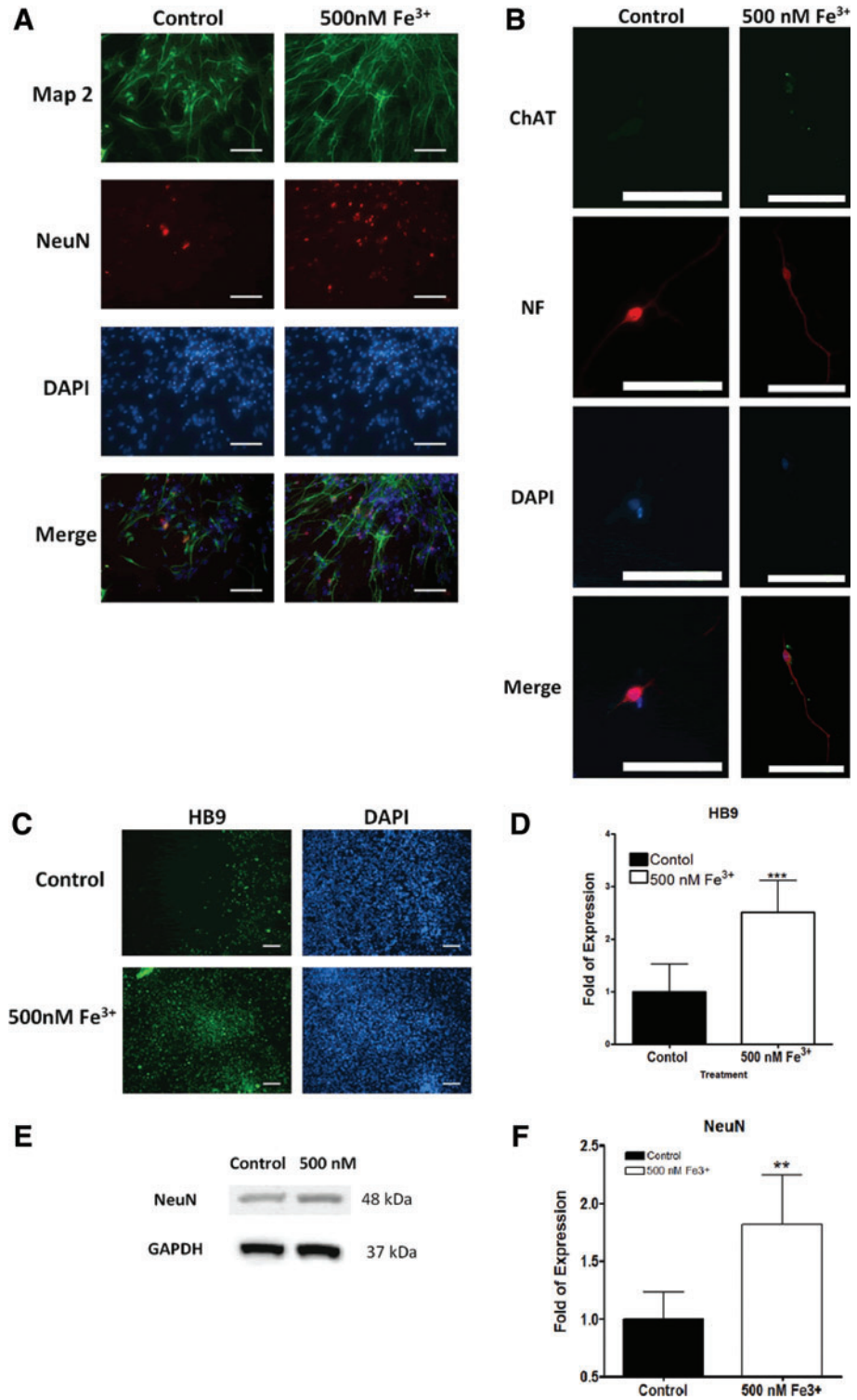
and the control samples (Fig. 1E). Figure 1E is also well corroborated by the peripherin data from Figure 2B and C.

*Further neuronal maturation of elevated iron concentration accelerated cells in neurobasal medium*

Knowing that iron accelerated neuronal differentiation, we subsequently investigated whether elevated iron levels

could hasten cellular maturation. We subjected differentiated neuron-like cells, previously cultivated in iron-enriched N2 media for 5 days, in neurobasal medium (NBM)<sup>33</sup> for an additional 3 days. The 0.5 μM iron-treated neuronal cells developed more abundant MAP2 and NeuN expressions in NBM in contrast to control (Fig. 3A). According to western blotting data, NeuN expression is ~1.8-fold higher in the iron supplement groups than the

**FIG. 3.** Iron induces maturation of hESC-derived neurons. Immunofluorescent staining of mature neuron makers (A) NeuN (red), Map2 (green), and DAPI (blue) and (B) choline acetyltransferase (ChAT; green), neurofilament (NF; red) for the control, and 500 nM Fe<sup>3+</sup> (scale bar=40 μm). (C) Immunofluorescent staining of mature motor neurons expressing HB9 in the control and 500 nM Fe<sup>3+</sup> (scale bar=100 μm) with (D) expression of HB9/DAPI (n ≥ 17, \*\*\*p < 0.001). (E) Western blot analysis of NeuN with the (F) quantitative analysis of NeuN protein expression folds of increase for control and 500 nM Fe<sup>3+</sup> (n ≥ 3, \*\*p < 0.005). Color images available online at [www.liebertpub.com/tec](http://www.liebertpub.com/tec)



control (Fig. 3E, F). Our data indicated that higher iron concentrations fostered maturation of differentiated neurons within 8 days of differentiation. With establishment of iron-enriched acceleration in neuronal differentiation and maturation, we further investigated whether it preferentially promoted a motor neuron lineage. After cultured in NBM for 3 days, cells previously treated with 0.5  $\mu\text{M}$  iron were positively stained with biomarkers, including ChAT, NF, and HB9,<sup>8</sup> characteristics of matured motor neurons (Fig. 3B–D). Quantitative immunofluorescence measurement of HB9 expression also unveiled  $\sim 2.5$ -fold upregulation in iron-enriched cultures comparing with the control (Fig. 3D).

#### Neuronal functional assay

With Figure 4A showing positive colocalized Synapsin I and  $\beta$ -III tubulin expression, our next step examined the functionality of the derived motor neurons with FM 1–43 dye to label active synaptic vesicles.<sup>36</sup> High potassium ( $\text{K}^+$ ) buffer was used to depolarize motor neurons and facilitate dye uptake. Physiological relevant agonists such as ACh, glutamic acid, and high potassium depolarization buffer were used to induce synaptic depolarization<sup>36</sup> (Fig. 4B, C).

Synaptic depolarization stimulated with ACh, glutamic acid, and high  $\text{K}^+$  was drastically apparent in the 0.5  $\mu\text{M}$   $\text{Fe}^{3+}$  group. Our results suggest that higher iron levels led to more mature and functional motor neuron-like cells with active synaptic vesicles.

#### Differential role of $\text{Fe}^{3+}$ and $\text{Fe}^{2+}$ in accelerating neuronal differentiation

Both ferric and ferrous forms can coexist in nature and in differentiation media. To explore the role of each ionic species that contributes to the acceleration,  $\text{Fe}^{3+}$  (0.5  $\mu\text{M}$ ),  $\text{Fe}^{2+}$  (0.5  $\mu\text{M}$ ), and the combination of the two (0.25  $\mu\text{M}$  of each) were examined separately.  $\text{Fe}^{3+}$  treatment clearly accelerated axonal sprouting by  $\sim 1.25$ -fold and enhanced axonal density by  $\sim 1.4$ -fold in comparison with the control (Fig. 5). On the contrary,  $\text{Fe}^{2+}$  seemed to foster inhibitory effects on axonal growth and slightly promoted axonal density (Fig. 5). The combinatory treatment of  $\text{Fe}^{3+}$  and  $\text{Fe}^{2+}$  substantially increased both sprouting density and axonal length (Fig. 5). Therefore, while both ionic species coexist in solution,  $\text{Fe}^{3+}$  ions played a more predominant role in the acceleration effect observed in this study.

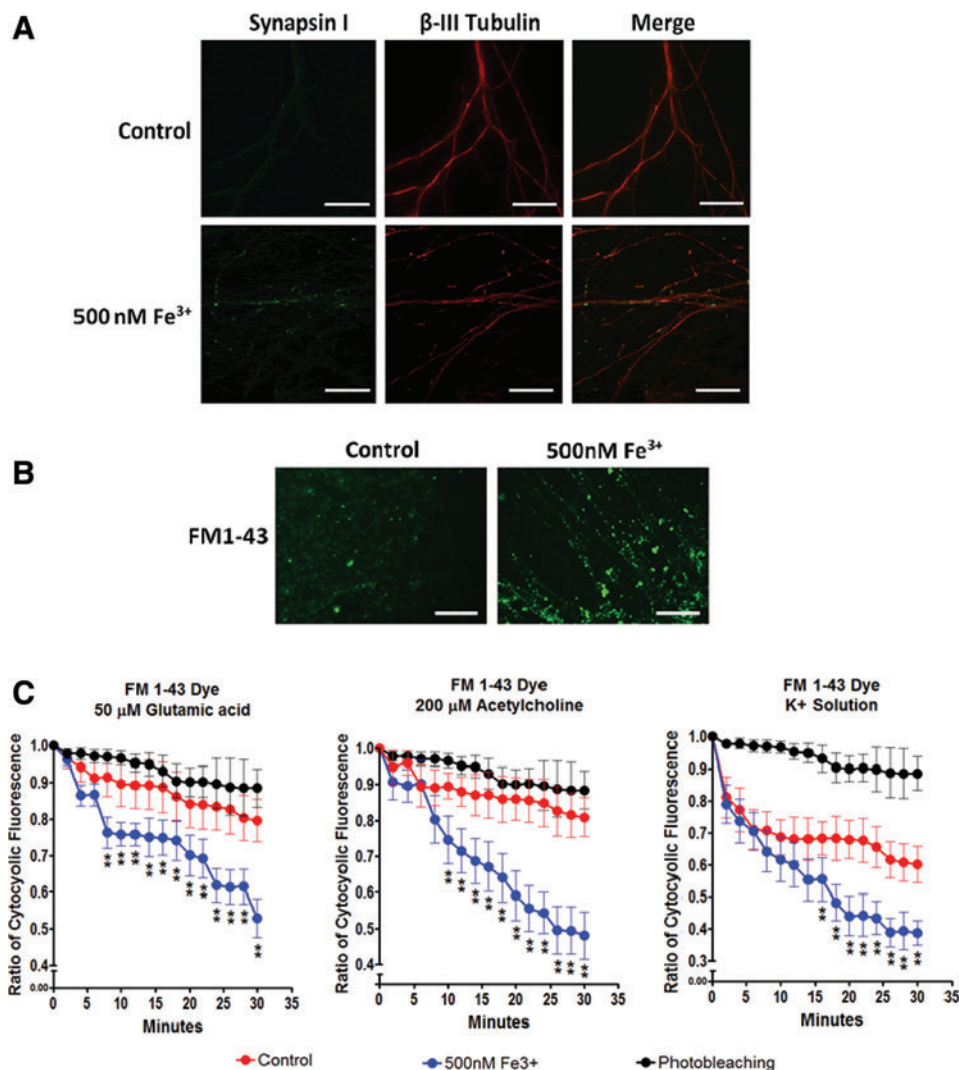


**FIG. 4.** Functional properties of hESC-derived motoneuron. (A) Confocal images of synapsin I and  $\beta$ -III tubulin colocalize staining (scale bar = 40  $\mu\text{m}$ ). (B) Synaptic vesicles loaded with FM1-43 Dye of the control and 500 nM  $\text{Fe}^{3+}$  (scale bar = 80  $\mu\text{m}$ ). (C) Cytocyclic fluorescence of the control (red circle) and 500 nM  $\text{Fe}^{3+}$  (blue circle) treatment groups loaded with FM1-43 dye and stimulated with 50  $\mu\text{M}$  glutamic acid, 200  $\mu\text{M}$  acetylcholine, and potassium (90 mM) solution to observe cell synaptic re-cycling responses to different natural agonist ( $n \geq 3$ ,  $**p < 0.005$ ). Photo bleaching was tested to normalize differences (black circle). Color images available online at [www.liebertpub.com/tec](http://www.liebertpub.com/tec)

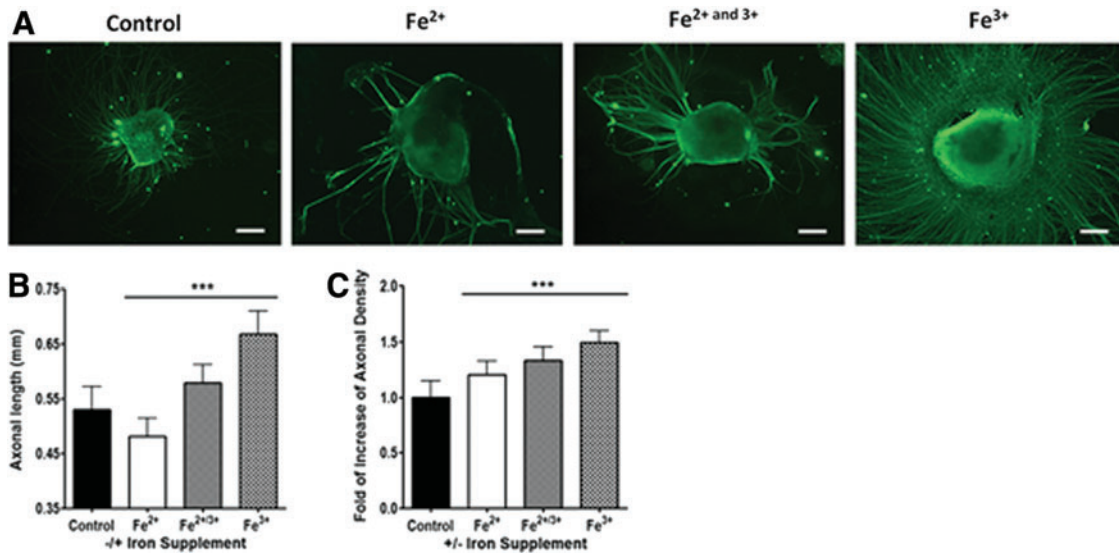


**FIG. 5.** Immunofluorescent staining of (A)  $\beta$ -III tubulin for hESC-differentiated neurons with  $\text{Fe}^{2+}$  ( $0.5 \mu\text{M}$ ),  $\text{Fe}^{3+}$  ( $0.5 \mu\text{M}$ ), and a combination of both solution ( $0.25 \mu\text{M}$  of  $\text{Fe}^{2+}/3+$  respectively) (scale bar =  $200 \mu\text{m}$ ). Analysis of the (B) axonal length (mm) ( $n \geq 100$ ,  $***p < 0.001$ ) and (C) axonal density on varying iron concentrations. Color images available online at [www.liebertpub.com/tec](http://www.liebertpub.com/tec)

#### Reactive oxidative species involvement in iron-induced acceleration

We then analyzed the partake of reactive oxidative species (ROS)<sup>37</sup> in determining accelerated differentiation.<sup>38</sup> N-acetyl-L-cysteine (NAC;  $1 \text{ mM}$ ) was added to  $\text{Fe}^{+3}$ -treated hESCs to block generation of ROS.<sup>39</sup> We found NAC treatment was not able to reduce acceleration or differentiation (Fig. 6A). The result suggested that ROS might not be involved in accelerating differentiation and that an alternative mechanism must be engaged. The data led to the postulation of an iron-mediated neuronal differentiation.

#### Transferrin mediated iron-induced acceleration

We postulated that an iron directed mechanism may be attributed to faster differentiation. By inhibiting granular acidification with methylamine chloride, transferrin-

mediated iron intake can be blocked.<sup>34,40</sup> Figure 6B showed that blocking transferrin pathway significantly attenuated axonal sprouting and density (Fig. 3). LysoSensor Green DND-189 (Invitrogen) was used to verify the effect of methylamine on vesicular acidification.<sup>34,41</sup> Methylamine effectively diminished the fluorescence of the LysoSensor Green DND-189 by disrupting granular pH (Fig. 7). Our data suggested that accelerated neuronal differentiation is clearly related to a transferrin-mediated mechanism.

#### Discussion

Motor neuron diseases are a group of life-threatening neurological disorders that are characterized by progressive motor neuron degeneration.<sup>42-44</sup> Recent studies have suggested that stem cell-derived motor neuron transplantation may be a promising therapy. This emergent strategy has been

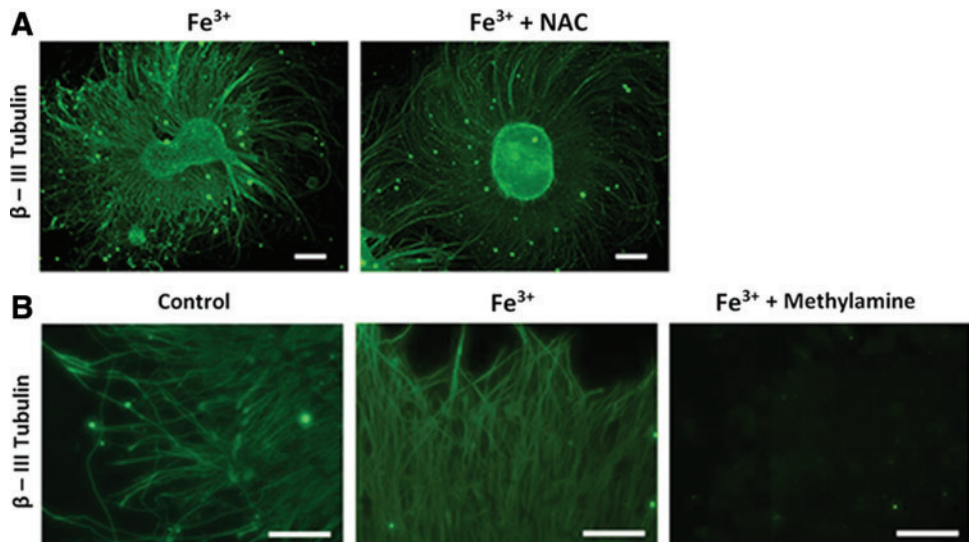


**FIG. 6.** Reactive oxidative species and transferrin inhibition in iron induced hESC-derived neurons. (A) hESC cultured with N-acetyl-L-cysteine (NAC;  $1 \text{ mM}$ ) in both control and  $500 \text{ nM}$   $\text{Fe}^{3+}$  groups stained with  $\beta$ -III tubulin (green) (scale bar =  $200 \mu\text{m}$ ) and (B) methylamine treated ( $100 \mu\text{M}$ ) hESC expressing  $\beta$ -III tubulin (green) (scale bar =  $80 \mu\text{m}$ ). Color images available online at [www.liebertpub.com/tec](http://www.liebertpub.com/tec)



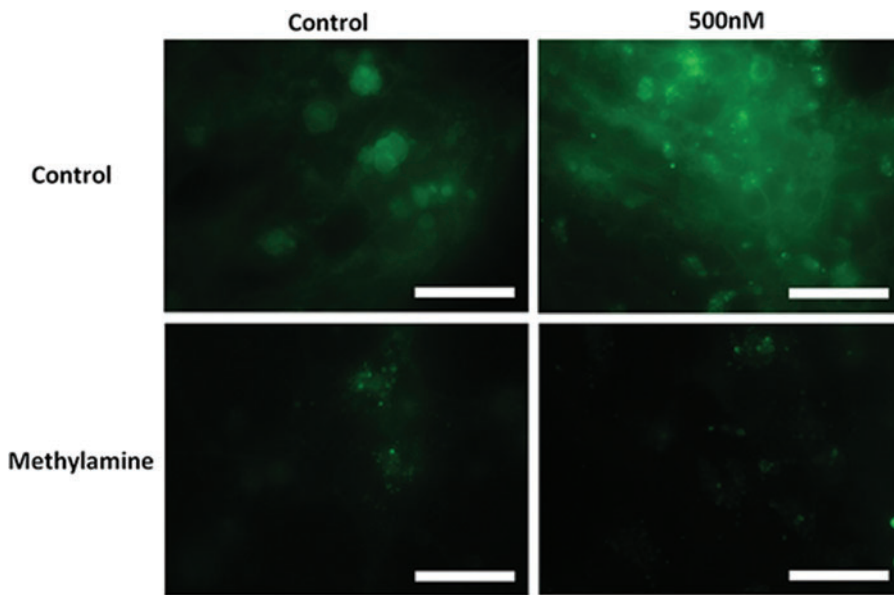


**FIG. 7.** Differentiated hESC loaded with LysoSensor™ Green DND-189 to observed granular pH within the cell. The control and 500 nM  $\text{Fe}^{3+}$  treatment groups were treated with methylamine hydrochloride (100  $\mu\text{M}$ ) to observe the increase in granular pH, reducing the fluorescence of the Lyso-Sensor Green DND-189 (scale bar = 12  $\mu\text{m}$ ). Color images available online at [www.liebertpub.com/tec](http://www.liebertpub.com/tec)

authenticated by solid *in vivo* efficacy and bears potential clinical relevance. Despite the potential as an effective therapy, the usage of costly neurotrophic factors seriously restricts motor neuron accessibility and expandability, and consequently hampers translational capacity. Thus, a cost-effective derivation method is desperately needed. Our previous discoveries reported how biochemical and physical cues could successfully promote neural differentiation. Here we presented the unexpected finding that increasing ferric availability to hESC hastened neuronal-specific motor neuron differentiation and enhanced the final yield.

To date, generation of motor neurons from hESC necessitates a continuous incubation with multiple doses of transcription activators and growth factors over a month to express matured motor neuron markers, that is, HB9.<sup>5,8,10,45</sup> Contrary to conventional methodology, our innovative protocol generated HB9 positive motor neurons in under 2 weeks, without RA or SHH, by increasing the iron concentration. According to immunofluorescence staining, 500 nM  $\text{Fe}^{3+}$  significantly raised HB9 expression (terminally differentiated motor neuron marker) by  $\sim 2.5$ -folds compared with control (Fig. 3C, D). Higher ferric concentration also engendered more matured motor neuron markers including synapsin and FM1-43-positive vesicles when compared with control (Fig. 4A, B). Colocalized staining of Synapsin I with  $\beta$ III tubulin and ChAT with NF further suggested the presence of neurotransmitter vesicles (Figs. 3B, 4A, and 4B). Besides the signature HB9 expression, we further assessed the function of derived motor neurons. Figure 4C showed that 500 nM  $\text{Fe}^{3+}$  treatment groups were drastically more responsive to active synaptic depolarization than control, when stimulated with physiological agonists including ACh, glutamic acid, and high  $\text{K}^+$ . Our findings are corroborated by previous studies showing that iron could encourage proliferation and differentiation of epidermal keratinocytes, dermal fibroblasts, and epidermal and dermal melanocytes in the skin of newborn mice.<sup>46</sup> In addition, higher ferric concentrations instigated oligodendrocyte differentiation from glial-restricted precursor cells.<sup>27</sup> Interestingly, our data authenticated for the first time that

increasing iron availability accelerated motor neuron differentiation, maturity, and functionality.

To understand the mechanism involved in accelerated motor neuron differentiation, we investigated the rate of neuronal differentiation from hESC under elevated iron concentration. The iron concentration range used in the study (0.1–1  $\mu\text{M}$ ) did not cause significant cellular toxicity (Figs. 1 and 2). By augmenting iron level in differentiation media, a concentration-dependent increase in  $\beta$ III tubulin and peripherin expressions, axonal length, and density was witnessed (Figs. 1 and 2) where most of the increase occurred relatively early between 5–8 days. Moreover, 500 nM  $\text{Fe}^{3+}$  significantly amplified matured neuronal makers such as NeuN and Map2 (Fig. 3A). These phenomena indicated that raising ferric concentration considerably accelerated hESC differentiation by rapidly committing to neural lineage, which precedes motor neuron derivation. Among various molecular mechanisms proposed, one of the prominent pathways involves generation of ROS and changing redox state of cells. Redox active iron may catalyze the formation of intracellular hydroxyl radicals through Fenton reaction in many cells including epithelium and neurons.<sup>37,44,47–49</sup> Intracellular ROS level and signaling closely modulate early neural development and can promote O-2A progenitor cells differentiating into oligodendrocytes.<sup>37,44,49,50</sup> We surmised that the iron-instigated accelerated neuronal differentiation could follow a similar pathway. Surprisingly, treatment with NAC, a common antioxidant, failed to inhibit accelerated neuronal differentiation and subsequent motor neuron development (Fig. 6A). The evidence suggested that iron-mediated ROS does not play a major role in accelerating neuronal differentiation and motor neuron maturation. Hence, an alternative mechanism may be involved.

We then hypothesized that iron could directly influence neuronal differentiation via transferrin-mediated pathway. After binding to iron, diferric holo-transferrin attaches to transferrin receptor forming a complex, which is subsequently endocytosed into early endosome.<sup>51</sup> The acidic vesicular with pH 5.5 then induces a conformational change between the complex, releasing iron from transferrin into vesicles.<sup>51</sup> To validate the

involvement of transferrin pathway, 500 nM Fe<sup>+</sup> treatment escalated the number of low pH vesicles as indicated by the brightly fluorescent spots (Fig. 7), implying increased formation of transferrin complex in endosomes.<sup>52,53</sup> Raising the vesicular pH with methylamine, disturbed the transferrin mechanism and subsequently disabled neuronal differentiation and significantly eliminated axonal sprouting and motor neuron formation (Fig. 7). While there are other types of iron chelators/inhibitors that can block cellular iron uptake, methylamine is commonly used to inhibit intercellular iron transport.<sup>34,54–56</sup> Our results are further supported by the well-established transferrin-ferritin intracellular iron transport and storage mechanism.<sup>53</sup> Additional evidences showed that the predominant proteins, upregulated during neural stem cell differentiation, involved in iron storage (ferritin L chain) and cytoskeleton.<sup>57</sup> In particular, ferritin can bind to microtubules, using them to transport and distribute cytosolic iron for further metabolism that is vital for cytoskeletal rearrangement.<sup>58</sup> Ferritin is also associated with the secretion of BDNF known to promote motor neuron differentiation.<sup>59,60</sup> Since elevating extracellular iron concentration can increase cytosolic ferritin,<sup>61</sup> it is implicative that increasing iron availability accelerates neuronal differentiation of hESC into motor neuron by increasing ferritin and BDNF. Conversely, perinatal iron deficiency in rats decreases BDNF and IGF levels, which may lead to reduced neuronal proliferation, differentiation, dendritic complexity, and impaired synaptic plasticity.<sup>23</sup> Such insufficiencies place a developmental brake on neural structures and underscore the importance of iron homeostasis in modulating neurotrophic factors critical for early-life neural differentiation.<sup>23</sup> It would be of interest to understand whether iron-accelerated hESC differentiation to motor neuron involves ferritin, BDNF, and IGF, and the possible downstream cellular signaling pathways.

In addition to stimulating the secretion of growth factors, iron homeostasis is intimately coupled to energy metabolism and neural developments.<sup>62,63</sup> Iron facilitates the generation of energy (ATP) by acting as a cofactor for cytochromes and Fe-sulfur complexes during oxidative phosphorylation.<sup>27</sup> High energy-dependent processes, such as neuronal differentiation, neurotransmission, and neuronal dendrite developments, are significantly compromised under iron deprivation.<sup>64,65</sup> Since transferrin-mediated iron transport may be a vital mechanism, we analyzed transferrin's role in shuttling extracellular ferrous ions, ferric ions, and a mixture of both. Ferric iron was significantly more effective in accelerating axonal extension and density, and motor neuron differentiation than ferrous alone or mixture (Fig. 5). These results lent support to the possible notion that transferrin transports ferric ions to hasten neuronal differentiation from hESC toward motor neurons. Other reports aligned well with our discovery documenting that ferrous ions can be more toxic to neuronal cells than ferric form by possibly inducing membrane peroxidation through ROS,<sup>66</sup> and it may reduce proliferation of differentiating neuroprogenitor cells.<sup>67</sup> Moreover, ferric ionic state successfully promoted Schwann cell and osteoclast differentiation.<sup>68,69</sup> These phenomena may help explain why transferrin and ferric ions play indispensable roles in driving motor neuron differentiation.

## Conclusion

In this study, we investigated the role of iron in motor neuron differentiation from hESC. We have demonstrated

that increasing the iron availability accelerated motor neuron-like differentiation and maturity. The H9-derived cells display some motor neuron characteristics and are functional that exhibits synaptic recycling capacities. This cost-effective protocol capitalizing on altering ionic concentrations significantly expedites the mass production of differentiated neurons for patients in need of neuronal regenerative therapy and can be potentially modified to accelerate the yield of multiple neuronal lineages.

## Acknowledgments

This study was supported in part by grants from the Muscular Dystrophy Association (MDA) and Linkou Chang Gung Memorial Hospital (CMRPD1C0031).

## Disclosure Statement

No competing financial interests exist.

## References

- Shelton, F.N., and Reding, M.J. Effect of lesion location on upper limb motor recovery after stroke. *Stroke* **32**, 107, 2001.
- Arvidsson, A., Collin, T., Kirik, D., Kokaia, Z., and Lindvall, O. Neuronal replacement from endogenous precursors in the adult brain after stroke. *Nature Med* **8**, 963, 2002.
- Kondziolka, D., Wechsler, L., Goldstein, S., Meltzer, C., Thulborn, K., Gebel, J., *et al.* Transplantation of cultured human neuronal cells for patients with stroke. *Neurology* **55**, 565, 2000.
- Lindvall, O., and Kokaia, Z. Stem cells for the treatment of neurological disorders. *Nature* **441**, 1094, 2006.
- Hu, B.Y., and Zhang, S.C. Differentiation of spinal motor neurons from pluripotent human stem cells. *Nat Protoc* **4**, 1295, 2009.
- Stacpoole, S.R., Bilican, B., Webber, D.J., Luzhynskaya, A., He, X.L., Compston, A., *et al.* Efficient derivation of NPCs, spinal motor neurons and midbrain dopaminergic neurons from hESCs at 3% oxygen. *Nat Protoc* **6**, 1229, 2011.
- Erceg, S., Ronaghi, M., and Stojkovic, M. Human embryonic stem cell differentiation toward regional specific neural precursors. *Stem Cells* **27**, 78, 2009.
- Li, X.J., Du, Z.W., Zarnowska, E.D., Pankratz, M., Hansen, L.O., Pearce, R.A., *et al.* Specification of motoneurons from human embryonic stem cells. *Nat Biotechnol* **23**, 215–221, 2005.
- Axell, M.Z., Zlateva, S., and Curtis, M. A method for rapid derivation and propagation of neural progenitors from human embryonic stem cells. *J Neurosci Methods* **184**, 275, 2009.
- Wichterle, H., Lieberam, I., Porter, J.A., and Jessell, T.M. Directed differentiation of embryonic stem cells into motor neurons. *Cell* **110**, 385, 2002.
- Gertz, C.C., Leach, M.K., Birrell, L.K., Martin, D.C., Feldman, E.L., and Corey, J.M. Accelerated neurogenesis and maturation of primary spinal motor neurons in response to nanofibers. *Dev Neurobiol* **70**, 589, 2010.
- Vodouhe, C., Schmittbuhl, M., Boulmedais, F., Bagnard, D., Vautier, D., Schaaf, P., *et al.* Effect of functionalization of multilayered polyelectrolyte films on motoneuron growth. *Biomaterials* **26**, 545, 2005.
- Moolenaar, W.H., Tsien, R.Y., Van der Saag, P.T., and De Laat, S.W. Na<sup>+</sup>/H<sup>+</sup> exchange and cytoplasmic pH in the

- action of growth factors in human fibroblasts. *Nature* **304**, 645, 1983.
14. Quinn, D.A., Dahlberg, C.G., Bonventre, J.P., Scheid, C.R., Honeyman, T., Joseph, P.M., *et al.* The role of Na<sup>+</sup>/H<sup>+</sup> exchange and growth factors in pulmonary artery smooth muscle cell proliferation. *Am J Respir Cell Mol Biol* **14**, 139, 1996.
  15. Hennings, H., Michael, D., Cheng, C., Steinert, P., Holbrook, K., and Yuspa, S.H. Calcium regulation of growth and differentiation of mouse epidermal cells in culture. *Cell* **19**, 245, 1980.
  16. Sage, H., Vernon, R.B., Funk, S.E., Everitt, E.A., and Angello, J. SPARC, a secreted protein associated with cellular proliferation, inhibits cell spreading *in vitro* and exhibits Ca<sup>2+</sup>-dependent binding to the extracellular matrix. *J Cell Biol* **109**, 341, 1989.
  17. MacDonald, R.S. The role of zinc in growth and cell proliferation. *J Nutr* **130**, 1500S, 2000.
  18. Beyersmann, D., and Haase, H. Functions of zinc in signaling, proliferation and differentiation of mammalian cells. *Biometals* **14**, 331, 2001.
  19. Hirobe, T. Ferrous ferric chloride stimulates the proliferation of human skin keratinocytes, melanocytes, and fibroblasts in culture. *J Health Sci* **55**, 447, 2009.
  20. Cazzola, M., Bergamaschi, G., Dezza, L., and Arosio, P. Manipulations of cellular iron metabolism for modulating normal and malignant cell proliferation: achievements and prospects. *Blood* **75**, 1903, 1990.
  21. Meguro, R., Asano, Y., Odagiri, S., Li, C., and Shoumura, K. Cellular and subcellular localizations of nonheme ferric and ferrous iron in the rat brain: a light and electron microscopic study by the perfusion-Perls and -Turnbull methods. *Arch Histol Cytol* **71**, 205, 2008.
  22. Sadrzadeh, S.M., and Saffari, Y. Iron and brain disorders. *Am J Clin Pathol* **121 Suppl**, S64, 2004.
  23. Tran, P.V., Carlson, E.S., Fretham, S.J., and Georgieff, M.K. Early-life iron deficiency anemia alters neurotrophic factor expression and hippocampal neuron differentiation in male rats. *J Nutr* **138**, 2495, 2008.
  24. Li, Y., Kim, J., Buckett, P.D., Bohlke, M., Maher, T.J., and Wessling-Resnick, M. Severe postnatal iron deficiency alters emotional behavior and dopamine levels in the prefrontal cortex of young male rats. *J Nutr* **141**, 2133, 2011.
  25. O'Keeffe, S.T., Gavin, K., and Lavan, J.N. Iron status and restless legs syndrome in the elderly. *Age Ageing* **23**, 200, 1994.
  26. Krieger, J., and Schroeder, C. Iron, brain and restless legs syndrome. *Sleep Med Rev* **5**, 277, 2001.
  27. Todorich, B., Pasquini, J.M., Garcia, C.I., Paez, P.M., and Connor, J.R. Oligodendrocytes and myelination: the role of iron. *Glia* **57**, 467, 2009.
  28. Cheng, A., Hou, Y., and Mattson, M.P. Mitochondria and neuroplasticity. *ASN Neuro* **2**, e00045, 2010.
  29. Chao, T.I., Xiang, S., Chen, C.S., Chin, W.C., Nelson, A.J., Wang, C., *et al.* Carbon nanotubes promote neuron differentiation from human embryonic stem cells. *Biochem Biophys Res Commun* **384**, 426, 2009.
  30. Chen, E.Y.T., Wang, Y.-C., Mintz, A., Richards, A., Chen, C.-S., Lu, D., *et al.* Activated charcoal composite biomaterial promotes human embryonic stem cell differentiation toward neuronal lineage. *J Biomed Mater Res Part A* **100A**, 2006, 2012.
  31. Zhang, S.C., Wernig, M., Duncan, I.D., Brustle, O., and Thomson, J.A. *In vitro* differentiation of transplantable neural precursors from human embryonic stem cells. *Nat Biotechnol* **19**, 1129, 2001.
  32. Pankratz, M.T., Li, X.J., LaVaute, T.M., Lyons, E.A., Chen, X., and Zhang, S.C. Directed neural differentiation of human embryonic stem cells via an obligated primitive anterior stage. *Stem Cells* **25**, 1511, 2007.
  33. Nguyen, T., Mehta, N.R., Conant, K., Kim, K.-J., Jones, M., Calabresi, P.A., *et al.* Axonal protective effects of the myelin-associated glycoprotein. *J Neurosci* **29**, 630, 2009.
  34. Swaiman, K.F., and Machen, V.L. Iron uptake by mammalian cortical neurons. *Ann Neurol* **16**, 66, 1984.
  35. Dyson, S.E., and Jones, D.G. Synaptic remodelling during development and maturation: junction differentiation and splitting as a mechanism for modifying connectivity. *Dev Brain Res* **13**, 125, 1984.
  36. Ryan, T.A., Reuter, H., Wendland, B., Schweizer, F.E., Tsien, R.W., and Smith, S.J. The kinetics of synaptic vesicle recycling measured at single presynaptic boutons. *Neuron* **11**, 713, 1993.
  37. Zecca, L., Youdim, M.B.H., Riederer, P., Connor, J.R., and Crichton, R.R. Iron, brain ageing and neurodegenerative disorders. *Nat Rev Neurosci* **5**, 863, 2004.
  38. Suzukawa, K., Miura, K., Mitsushita, J., Resau, J., Hirose, K., Crystal, R., *et al.* Nerve growth factor-induced neuronal differentiation requires generation of Rac1-regulated reactive oxygen species. *J Biol Chem* **275**, 13175, 2000.
  39. Zafarullah, M., Li, W.Q., Sylvester, J., and Ahmad, M. Molecular mechanisms of N-acetylcysteine actions. *Cell Mol Life Sci* **60**, 6, 2003.
  40. Qian, Z.M., and Shen, X. Brain iron transport and neurodegeneration. *Trends Mol Med* **7**, 103, 2001.
  41. Barg, S., Huang, P., Eliasson, L., Nelson, D.J., Obermüller, S., Rorsman, P., *et al.* Priming of insulin granules for exocytosis by granular Cl<sup>-</sup> uptake and acidification. *J Cell Sci* **114**, 2145, 2001.
  42. Leigh, P.N., and Ray-Chaudhuri, K. Motor neuron disease. *J Neurol Neurosurg Psychiatry* **57**, 886, 1994.
  43. Mulder, D.W., Kurland, L.T., Offord, K.P., and Beard, C.M. Familial adult motor neuron disease: amyotrophic lateral sclerosis. *Neurology* **36**, 511, 1986.
  44. Altamura, S., and Muckenthaler, M.U. Iron toxicity in diseases of aging: Alzheimer's disease, Parkinson's disease and atherosclerosis. *J Alzheimer Dis* **16**, 879, 2009.
  45. Miles, G.B., Yohn, D.C., Wichterle, H., Jessell, T.M., Rafuse, V.F., and Brownstone, R.M. Functional properties of motoneurons derived from mouse embryonic stem cells. *J Neurosci* **24**, 7848, 2004.
  46. Hirobe, T. Ferrous ferric chloride induces the differentiation of cultured mouse epidermal melanocytes additionally with herbal medicines. *J Health Sci* **55**, 86, 2009.
  47. Dringen, R., Bishop, G.M., Koeppe, M., Dang, T.N., and Robinson, S.R. The pivotal role of astrocytes in the metabolism of iron in the brain. *Neurochem Res* **32**, 1884, 2007.
  48. Britton, R.S., Leicester, K.L., Bacon BR. Iron toxicity and chelation therapy. *Int J Hematol* **76**, 219, 2002.
  49. Todorich, B., Zhang, X., and Connor, J.R. H-ferritin is the major source of iron for oligodendrocytes. *Glia* **59**, 927, 2011.
  50. Smith, J., Ladi, E., Mayer-Proschel, M., and Noble, M. Redox state is a central modulator of the balance between self-renewal and differentiation in a dividing glial precursor cell. *Proc Natl Acad Sci U S A* **97**, 10032, 2000.
  51. Zhang, D., Lee, H.F., Pettit, S.C., Zaro, J.L., Huang, N., and Shen, W.C. Characterization of transferrin receptor-mediated

- endocytosis and cellular iron delivery of recombinant human serum transferrin from rice (*Oryza sativa* L.). *BMC Biotechnol* **12**, 92, 2012.
52. Dautry-Varsat, A., Ciechanover, A., and Lodish, H.F. pH and the recycling of transferrin during receptor-mediated endocytosis. *Proc Natl Acad Sci U S A* **80**, 2258, 1983.
  53. Dautry-Varsat, A. Receptor-mediated endocytosis: the intracellular journey of transferrin and its receptor. *Biochimie* **68**, 375, 1986.
  54. Paterson, S., Armstrong, N.J., Iacopetta, B.J., McArdle, H.J., and Morgan, E.H. Intravesicular pH and iron uptake by immature erythroid cells. *J Cell Physiol* **120**, 225, 1984.
  55. Levi, A., Shechter, Y., Neufeld, E.J., and Schlessinger, J. Mobility, clustering, and transport of nerve growth factor in embryonal sensory cells and in a sympathetic neuronal cell line. *Proc Natl Acad Sci U S A* **77**, 3469, 1980.
  56. Bomford, A., Young, S.P., and Williams, R. Release of iron from the two iron-binding sites of transferrin by cultured human cells: modulation by methylamine. *Biochemistry* **24**, 3472, 1985.
  57. Skalnikova, H., Halada, P., Vodicka, P., Motlik, J., Rehulka, P., Horning, O., *et al.* A proteomic approach to studying the differentiation of neural stem cells. *Proteomics* **7**, 1825, 2007.
  58. Hasan, M.R., Koikawa, S., Kotani, S., Miyamoto, S., and Nakagawa, H. Ferritin forms dynamic oligomers to associate with microtubules *in vivo*: implication for the role of microtubules in iron metabolism. *Exp Cell Res* **312**, 1950, 2006.
  59. Schonberg, D.L., Goldstein, E.Z., Sahinkaya, F.R., Wei, P., Popovich, P.G., and McTigue, D.M. Ferritin stimulates oligodendrocyte genesis in the adult spinal cord and can be transferred from macrophages to NG2 cells *in vivo*. *J Neurosci* **32**, 5374, 2012.
  60. Koliatsos, V.E., Clatterbuck, R.E., Winslow, J.W., Cayouette, M.H., and Price, D.L. Evidence that brain-derived neurotrophic factor is a trophic factor for motor neurons *in vivo*. *Neuron* **10**, 359, 1993.
  61. Casey, J.L., Hentze, M.W., Koeller, D.M., Caughman, S.W., Rouault, T.A., Klausner, R.D., *et al.* Iron-responsive elements: regulatory RNA sequences that control mRNA levels and translation. *Science* (New York, NY) **240**, 924, 1988.
  62. Rouault, T.A. The role of iron regulatory proteins in mammalian iron homeostasis and disease. *Nat Chem Biol* **2**, 406, 2006.
  63. Hentze, M.W., Muckenthaler, M.U., and Andrews, N.C. Balancing acts: molecular control of mammalian iron metabolism. *Cell* **117**, 285, 2004.
  64. Beard, J.L. Iron biology in immune function, muscle metabolism and neuronal functioning. *J Nutr* **131**, 568S, 2001.
  65. Benarroch, E.E. Brain iron homeostasis and neurodegenerative disease. *Neurology* **72**, 1436, 2009.
  66. Singh, A.V., Vyas, V., Montani, E., Cartelli, D., Parazzoli, D., Oldani, A., *et al.* Investigation of *in vitro* cytotoxicity of the redox state of ionic iron in neuroblastoma cells. *J Neurosci Rural Pract* **3**, 301, 2012.
  67. Mazur-Kolecka, B., Cohen, I.L., Jenkins, E.C., Flory, M., Merz, G., Ted Brown, W., *et al.* Sera from children with autism alter proliferation of human neuronal progenitor cells exposed to oxidation. *Neurotox Res* **16**, 87, 2009.
  68. Salis, C., Davio, C., Usach, V., Urtasun, N., Goitia, B., Martinez-Vivot, R., *et al.* Iron and holotransferrin induce cAMP-dependent differentiation of Schwann cells. *Neurochem Int* **61**, 798, 2012.
  69. Jia, P., Xu, Y.J., Zhang, Z.L., Li, K., Li, B., Zhang, W., *et al.* Ferric ion could facilitate osteoclast differentiation and bone resorption through the production of reactive oxygen species. *J Orthop Res* **30**, 1843, 2012.

Address correspondence to:

Wei-Chun Chin, PhD  
 Bioengineering Program  
 School of Engineering  
 University of California  
 5200 North Lake Road  
 Merced, CA 95343

E-mail: wchin2@ucmerced.edu

Received: December 3, 2013

Accepted: July 10, 2014

Online Publication Date: August 22, 2014